IOPscience iopscience.iop.org

Home Search Collections Journals About Contact us My IOPscience

Three-wave vibrational mode broadening for Fibonacci one-dimensional quasicrystals

This article has been downloaded from IOPscience. Please scroll down to see the full text article.

2005 J. Phys.: Condens. Matter 17 6849

(http://iopscience.iop.org/0953-8984/17/43/006)

View the table of contents for this issue, or go to the journal homepage for more

Download details:
IP Address: 129.252.86.83
The article was downloaded on 28/05/2010 at 06:35

Please note that terms and conditions apply.

INSTITUTE OF PHYSICS PUBLISHING JOURNAL OF PHYSICS: CONDENSED MATTER

J. Phys.: Condens. Matter **17** (2005) 6849–6869 doi:10.1088/0953-8984/17/43/006

Three-wave vibrational mode broadening for Fibonacci one-dimensional quasicrystals

E I Kats[1,2] **and A R Muratov**[1,3]

[1] Laue-Langevin Institute, F-38042, Grenoble, France
[2] L D Landau Institute for Theoretical Physics, RAS, 117940 GSP-1, Moscow, Russia
[3] Institute for Oil and Gas Research, Moscow, Russia

Received 8 June 2005, in final form 29 August 2005
Published 14 October 2005
Online at stacks.iop.org/JPhysCM/17/6849

Abstract

A one-dimensional Fibonacci chain is used to model vibrational mode broadening in icosahedral quasicrystals (i-QCs). All calculations are performed self-consistently for various finite size approximants at temperatures higher than the Debye temperature, T_D. This approach is extended to three-dimensional systems as well. It is shown that vibrational spectra depend crucially on the Fibonacci chain mass ratio m. For $m = 3$, which roughly mimics AlPdMn i-QC, there are three almost dispersionless optic modes separated from the acoustic mode by three large gaps, and for $m = 1/3$, which mimics ZnMgY i-QC, there is one dispersionless optic mode and one acoustic mode. For the first time we provide a qualitative model which predicts experimentally observed phonon spectrum broadening of i-QC. It is shown that three wave broadening for both one-dimensional and three-dimensional Fibonacci i-QCs is the leading mechanism of spectrum broadening. For the intermediate range of mode coupling constants, it scales with the mode frequency ω as $c_1\omega + c_2\omega^2$ (where c_1 and c_2 are some numerical constants). For smaller values of the coupling constant, phonon broadening is proportional to ω^3. We conclude that for a system with a non-simple elementary cell, vibrational spectrum broadening is always larger than for a system with a primitive cell (provided all other characteristics are the same).

1. Introduction

Extensive experimental and theoretical work on quasi-periodic systems, i.e., materials which exhibit non-periodic long-range order, has revealed interesting new properties which are not possible either in periodic or in disordered systems (see for example, review articles [1–3], and references therein). One of the remarkable and unexplained features of QCs is the apparent conflict between the high structure quality of these materials and their vibrational excitations [4–7], which are rather reminiscent of those for disordered materials [8, 9]. Although there is a considerable literature discussing vibrational eigenmodes and related

 © 2005 IOP Publishing Ltd Printed in the UK

properties of QCs, and a number of numerical calculations have been published over the last 20 years, there is still a clear need for a simple theoretical model with predictions which can be directly tested experimentally. For instance, results of exact diagonalization of dynamical matrices at high symmetry points of the small Brillouin zone for corresponding QC approximants (see for example [10], and also [11] for decagonal QCs with two-dimensional quasi-periodicity) lead to very rich density of vibrational states including many different modes. However, there is still very limited agreement between these theoretical studies (usually valid at $T = 0$) and experiments [4, 5, 3, 6, 7], performed mainly at room temperature and above. In part this frustrating situation is just due to the lack of a qualitative model of the vibrations in QCs, and the main goal of this paper is geared towards the building of such a simple model. Our aim in this paper is based on the fact that many robust room-temperature features of the vibrational modes in QCs, experimentally testable by neutron methods, are not sensitive to the more delicate aspects of quasi-periodic systems, such as the hierarchical nature of gaps [10–13], or critical multifractal character of the states [14–16]. Aiming to rationalize published room-temperature inelastic scattering data, we propose a coarse-grained model description of QC vibrational mode broadening based on consideration of finite size approximants.

One comment is necessary here before proceeding. While ideal crystal mode broadening is an intrinsically anharmonic phenomenon, the mode eigenfrequency can be accurately determined in the harmonic approximation. In contrast, even in the ideal QCs, where vibrational modes are in critical states (multifractal modes [11]), there is harmonic broadening. However, this natural broadening at $T > T_D$ is small, and dominant contribution is given by more robust anharmonic three-wave (i.e., involving the smallest number of excitations) broadening. The three-wave broadening can be quite accurately analysed in the framework of finite size approximant approach.

Our motivations for this paper are twofold. First is a simple observation that a disallowed in conventional crystalline materials fifth-order rotational symmetry of i-QCs determines the unique golden ratio $(\sqrt{5}-1)/2$ of incommensurate length scales that defines the structure of all i-QCs. As we will show, many robust and experimentally testable features of the excitation spectra in i-QCs are sensitive to mainly this specific feature of the structure. Second, for the first time we provide a systematic procedure for handling vibrational mode broadening in QCs. To our knowledge such analysis of the eigenmode broadening in QCs has not been carried out thus far. Furthermore, although the broadening is often considered as a nuisance, it provides valuable information on QC physical properties and eigenmode structure.

The simplest model structure constructed by the golden ratio is the one-dimensional (1D) Fibonacci chain. Our aim is not to claim that all results we found for the Fibonacci 1D model necessarily hold for real 3D i-QC materials. Note, however, that studies of low-dimensional systems such as 1D Fibonacci chains are interesting for applications in their own right, and when properly interpreted and treated the 1D model yields quite reasonable values for a variety of measured quantities. Moreover, our calculations can be performed self-consistently not only in one dimension but also can be generalized for 3D QCs. We study the model within the regular expansion over the parameter $\epsilon = 1 - 1/m$, assuming formally that $\epsilon \ll 1$, where m is the mass ratio for an effective binary QC (see its definition below in section 2). Of course our simple model is only a zero approximation which may not have exact quantitative results but can lead to correct predictions of the shapes of the dispersion laws.

Our paper is organized as follows. In section 2 we describe our model and calculate its vibrational spectrum. In section 3 we compute the eigenfunctions, and in section 4 we find the mode broadening due to anharmonic three-wave coupling. Finally we review and discuss our results in section 5. In two appendices we collect some more specialized technical material required for the calculations of phonon line broadening. Anharmonic third-order processes

for the five-particle approximant to the infinite Fibonacci chain are presented in appendix A. The main problem to treat theoretically mode broadening in 3D or 2D systems is that in a QC there is no well-defined Brillouin zone [12, 13]. Luckily, for finite-temperature three-wave broadening, the integrals entering the expressions for the broadening are determined by a relatively broad range of wavevectors, not only in the vicinity of the boundary q_0 of the pseudo-Brillouin zone. We perform this calculation of the three-wave phonon broadening in the isotropic 3D system with q-space limited by the sphere $|\mathbf{q}| = q_0$, (which is a good approximation for highly symmetric elastic properties of i-QCs [17, 18]), and the results are presented in appendix B. A more realistic model will not affect our conclusions much, and transparency of treatment is worth a simplification. Those readers who are not very interested in mathematical derivations can skip these appendices and find all essential physical results in the main text of the paper.

2. Fibonacci model

As is well known, a regular periodic 1D lattice can be generated from one basic unit cell by simple translation. For the ideal periodic system the solution of the equation of motion is wavelike and the vibrational spectrum forms one or more vibrational bands. The density of state is singular near these band edges. In the opposite limit of the totally disordered lattice, the wavefunctions exhibit localization behaviour, and one has only a discrete spectrum. The quasi-periodic lattices we are interested in this paper are intermediate in this sense between ideally periodic and totally disordered systems. To generate a 1D quasi-periodic system one has to apply a more general procedure. One popular example, simple, albeit providing a good physical model for several alloys, is the so-called Fibonacci inflation rule. We are constructing the chain from particles with masses 1 and m starting from a particle mass 1 as seed and following the rule, specified by two numbers 1 and m in the sequence

$$1 \to 1, m \qquad \text{and} \qquad m \to 1.$$

This process gives successively

$$(1), (1, m), (1, m, 1), (1, m, 1, 1, m), \ldots, \tag{2.1}$$

and so forth such that the ratio (number of m)/(number of 1) approaches the golden mean value $\sigma \equiv (\sqrt{5} - 1)/2 \simeq 0.62$ (the same as for i-QCs) in the limit of long sequences. If we start from the particle with the mass m, the inflation rule symmetric to (2.1) can be used to generate a Fibonacci chain where the roles of majority and minority basis are exchanged.

To determine the phonon spectrum of the Fibonacci chain we have to solve the dynamic equation for every atom (u_i is the displacement of the ith atom):

$$m_i \frac{\mathrm{d}^2 u_i}{\mathrm{d}t^2} = 2u_i - u_{i-1} - u_{i+1}. \tag{2.2}$$

Here and below we employ units with elastic moduli equal to unity. Of course it is impossible to solve (2.2) analytically for an arbitrary chain, with more than four particles, therefore numerical methods should be used to investigate the system.

The computations can be performed in many ways. For example one can find the vibrational spectrum using the standard transfer matrix formalism [19, 20]. However, predominantly aiming to analyse mode broadening, we will use here another approach that seems to be more appropriate for our purposes. First of all it is more convenient instead of the infinite Fibonacci chain to study the finite chain of length N with zero boundary conditions for the displacements $u(N) = u(0) = 0$, and to have the spectrum for the infinite chain, the

results should be computed in the limit $N \to \infty$. For a conventional 1D crystal, i.e., $m = 1$, we easily obtain the well-known spectrum

$$\omega(n) = 2\sin(2\pi n/N). \tag{2.3}$$

In the long-wavelength limit, $\omega \to 0$, the details of the quasi-periodic structure do not play a significant role for vibrational spectra (unlike electronic spectra), and therefore we get in this limit the same spectrum (2.3). Evidently this is not the case for finite ω and $m \neq 1$.

To be more specific and in contact with real i-QCs, note that almost all known i-QCs are three-component alloys, for example, $Al_{68}^{27}Pd_{21}^{106}Mn_{11}^{55}$, $Zn_{60}^{65}Mg_{31}^{24}Y_{9}^{89}$, where superscripts indicate the mass number of the element and subscripts show the atomic concentration of the element in the alloy. Unfortunately with the Fibonacci chain we can mimic simply only two-component alloys. However, luckily the above-mentioned i-QC alloys roughly contain one light component and two heavy components, and for both i-QCs we have a mass ratio between the average heavy and the light component about 1:3.3 at the composition 68:32 for AlPdMn, and a mass ratio 1:2.8 at the composition 31:69 for ZnMgY. We conclude that the composition in both cases is not very different from the golden ratio; therefore, the Fibonacci chain approximation at least in this respect might serve quite reasonably.

To have a nontrivial solution for the particle displacements u_i, the eigenmode frequency ω must satisfy the eigenvalue equation. The equation, for example, in the transfer matrix technique, is the condition that the determinant of the product of N transfer matrices should be zero. This allows us to find the phonon spectrum of the Fibonacci chain easily (see e.g. [20, 19]). The spectrum has gaps which may be labelled by the so-called Bloch index $\kappa_s = (1/2)s\sigma \,(\mathrm{mod}.1)$ (σ is the golden mean ratio) and the size of the gaps decreases roughly with increasing s; for small energies, the gap size for phonons tends to zero faster than ω [10, 11, 17, 18]. The model exhibits characteristics of both regular periodic and disordered systems. In the low-frequency region, the system behaves as a regular periodic crystal (and the vibrational eigenfunctions appear extended); in the high-frequency region, there is no unique behaviour for the eigenfunctions, and the spectrum shows many gaps. However, the exact solution is, so to speak, too exact for our purposes, and contains too many subtle details of the model, and all branches of excitations simultaneously, while experimentally observed spectra measured at room temperature are much poorer, and it is not clear whether it is possible at all to observe or to test experimentally these theoretically predicted features of the spectra and somehow to find their characteristics. For i-QCs AlPdMn and ZnMgY, for which detailed studies have been carried out [4, 5, 3, 6, 7], vibrational excitation spectra can be separated into two well-defined regimes: the acoustic regime for frequencies smaller than 6–8 meV, and, for larger frequencies, a regime in which the dynamical response is characterized by a broad band of dispersionless optic-like modes. The optic-like spectrum generally consists of three or four broad bands (the width is of the order of few meV), and no any gap opening is observed. Therefore, aiming to understand underlying basic physics and to model even qualitatively observed dependences, one should not refine the model to include some additional mechanisms and details, but on the contrary, one has to coarse grain the model, to have a benchmark to compare theoretical predictions and experimental data.

Of course real i-QCs are not 1D Fibonacci chains. However, the 1D and 3D problems share a common mathematical foundation based on the golden mean ratio σ: both systems can be obtained by a projection method from a higher-dimensional space (2D square lattice for the Fibonacci model [21]), and it is not surprising that they have common robust and generic universal properties. As is the case in related electronic problems [22, 23], we expect the qualitative features of the spectra will carry over to 2D and 3D cases, and similar results hold for any irrational σ. Moreover, finite-temperature phonon line broadening, our main concern in

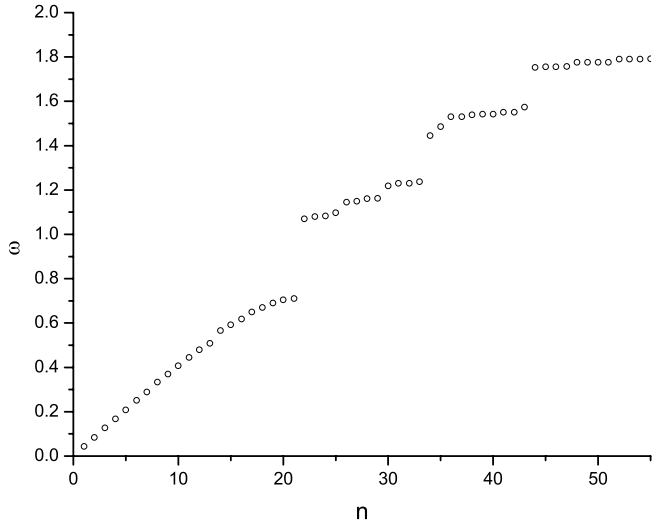

Figure 1. Spectrum for the Fibonacci chain with 55 particles in the elementary cell at zero displacement boundary conditions and for the mass ratio 1:3.

this paper, is an even more robust phenomenon in QCs than the spectrum itself. Indeed although mathematically in QCs we have to deal with infinitely many density modulation harmonics, filling the reciprocal space densely, most of these harmonics have very small amplitudes, and therefore only a few main harmonics taken into account in a finite size approximant dominate this kind of broadening. In our work we are mainly concerned with 1D Fibonacci chains; however, the aforesaid qualitative arguments also hold for 3D QCs (see appendix B where we have presented the generalization of our approach to 3D systems).

Let us recapitulate the results of our analysis of the 1D Fibonacci chain vibrational modes. The spectrum of the eigenmodes for 55 particles in the elementary cell shown in figure 1 was obtained for zero displacement boundary conditions and for the mass ratio 1:3. Evidently one can distinguish one acoustic branch and optical branches. Qualitatively the same features of the spectrum occur also for 233 or 1000 particles. Let us first consider the case when the mass ratio is about 1:3 and the composition is about 38:62, which can mimic i-QC AlPdMn. By a simple coarse-grained inspection of the calculation results we find that in this case we have three optical modes with rather weak dispersion, one acoustic mode and one quasi-optical mode next to the acoustic one. The gap between the acoustic branch and the first quasi-optical mode is much smaller than the other three gaps (cf with the exact numerical results [10, 11], and phenomenological analysis [17, 18]). Analogously for the composition 62:38, the spectrum has only two branches, one acoustic and one optic mode; the latter one is almost dispersionless (figure 2).

The zero boundary displacement conditions are widely used in the literature; see e.g. [20]. Such an approach is adequate if one determines the spectrum; however, the method is not suitable for the anharmonic three-wave mode broadening calculations. For example, in the limit $m = 1$, the eigenfunctions are simply sin-functions and the mean product of any three sin functions is always zero. For $m \neq 1$ this product is not zero anymore, but it is very small. Thus to analyse anharmonic contributions for the Fibonacci chain one must use a different approach.

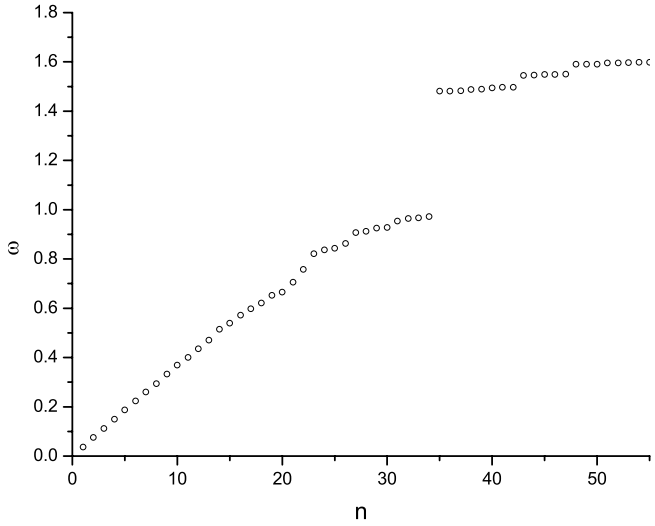

Figure 2. Spectrum of the Fibonacci sequence for mass ratio 3:1 (all other conditions and parameters are the same as in figure 1).

We can take some finite number (for example 5, which is the Fibonacci number) of the particles in the elementary cell and impose non-zero periodic boundary conditions, requiring that the corresponding quasi-momentum varies in the first Brillouin zone. Luckily it turns out that the spectrum calculated in this simple model in the harmonic approximation resembles the spectrum obtained by the previous method, although both spectra are expressed in different variables. Indeed, in the former approach the spectrum consists of discrete points and every mode can be uniquely characterized by an eigennumber, coinciding with the number of nodes of the eigenfunction [20], while in the latter approach the quasi-momentum plays the role of a wavevector which strictly speaking is undefined in the previous approach since in the Fibonacci model there is no periodicity and the Bloch states.

Eventually we have five modes (eigenfrequencies) which can be represented as the functions of the quasi-momentum. The fact that both spectra (i.e., those found for zero and non-zero boundary displacements) are close (see figure 3) is not an accidental coincidence. It is based on a natural coarse-grained generalization of the notion of wavevectors for the quasi-periodic systems. Further, we will show in the next section that in the limit of small frequencies the eigenfunctions of the Fibonacci chain vibrational spectrum are practically indistinguishable from Bloch-like waves. Thus one should expect that the quasi-momenta are reminiscent of the mode numbers. A similar behaviour is obtained for the next approximant in the series. As we proceed to the higher-order approximants, new gaps progressively appear in the spectrum, showing a hierarchical scaling structure. However, all coarse-grained global features of the spectrum remain the same as for very short approximants; in particular, the acoustic and optical modes we found above are very robust to the progressive fragmentation of the spectrum.

3. Eigenfunctions

For periodic systems, Bloch's theorem may be applied, and the solutions of (2.2) are propagating waves. In contrast, if the lattice is disordered, the eigenfunctions are localized,

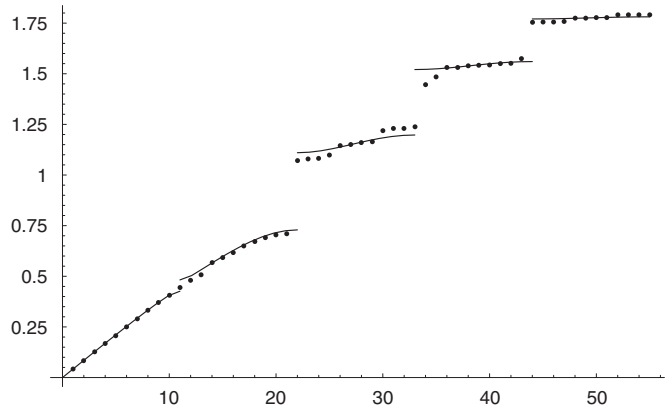

Figure 3. Comparison of the eigenspectra computed with zero displacement boundary conditions for the Fibonacci chain with 55 particles in the elementary cell (points) and with periodic boundary conditions for 5 particles in the elementary cell (solid line). The mass ratio is 1:3 for both cases; along the horizontal axis we put for the former case—mode number, and for the latter case—rescaled quasi-momentum.

and the spectrum is a discrete set of levels. Common sense suggests that since the Fibonacci chain is intermediate between periodic and disordered systems, it is expected to show both characteristics. Let us first consider the eigenfunctions for a discrete point-like spectrum (i.e., the eigenfrequency as the functions of the mode numbers). For small eigenfrequencies the eigenfunctions are similar to Bloch-like periodic functions. For the particular case of zero boundary conditions these eigenfunctions can be written as $\sin(\pi nx/L)$. Near the gaps the eigenfunctions are represented as certain linear combinations of the periodic functions, i.e., the wavepackets. The spectral width of any wavepacket is proportional to the value of the gap. The broadest eigenfunctions are at the boundaries of the gaps, and the values of the eigenfrequencies at the gaps are the corresponding Fibonacci numbers. We illustrate some features of the eigenfunctions in figure 4 where we present Fourier transforms of 5 typical eigenfunctions for a chain with 55 particles in the elementary cell. From this simple figure we conclude that (as it was already noted above) for small eigennumbers the eigenfunctions are not very different from periodic Bloch-like ones; however, near the gaps the eigenfunctions strongly deviate from the Bloch solutions and they describe localized or intermediate (critical) states.

To further clarify this situation a few remarks are in order.

- Since the eigenfunctions are not Bloch-like periodic ones, in the thermodynamic limit $N \to \infty$ there is no quasi-momentum conservation law.
- The eigenfunctions near large gaps have quite broad widths in reciprocal space; the spectral distributions of the neighbouring eigenfunctions are strongly overlapped. Having in mind neutron measurements this can lead to the situation when some phonon branches disappear at certain k-values and the next branch can appear at the lower quasi-momentum value.
- In all published inelastic single grain neutron scattering experiments [4–7], the predicted gaps in the vibrational spectra have not been detected. One can attribute this failure to the mode broadening, which can be larger than the corresponding gaps. The natural (i.e., harmonic) broadening, related to the fact that the calculated eigenfunctions have a finite width, is small and cannot close the big gaps between the optical modes. However, this natural broadening is predominant only at $T = 0$. At room temperature where inelastic

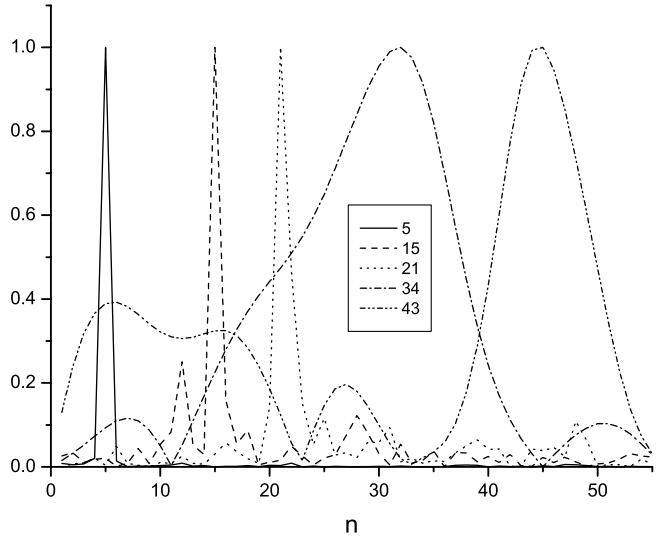

Figure 4. Fourier transforms of eigenfunctions with mode numbers 5, 15, 21, 34 and 43 for the zero displacement boundary conditions (the mass ratio is 1:3).

neutron scattering data are available, one has to include the other broadening mechanisms, and the most relevant and robust one is associated with three-phonon interactions [24]. A more realistic model with higher-order approximants will not affect our qualitative conclusions.

4. Three wave broadening

As was shown in the previous section, even five particles ordered as $1, m, 1, 1, m$ give the phonon spectrum qualitatively and semi-quantitatively quite close to the spectrum of the large Fibonacci chain. Evidently, for the five particles in the elementary cell system, one has five branches of the excitations: one acoustic branch (1), one optical mode (2) with non-zero dispersion close to the acoustical mode, and three optical almost dispersionless modes (3, 4, 5). For the mass ratio $m = 3$ the straightforward analysis of the spectrum (one has to compare merely the frequencies and wavevectors for the corresponding modes entering the processes) leads to the following anharmonic three-phonon processes satisfying energy and momentum conservation laws:

$$5 \leftrightarrow 4 + 1; \qquad 5 \leftrightarrow 3 + 2; \qquad 4 \leftrightarrow 3 + 1; \qquad 3 \leftrightarrow 2 + 2; \qquad 2 \leftrightarrow 1 + 1.$$

Here double arrows stand for the processes of decay and fusion of the corresponding excitation branches, for example, $2 \leftrightarrow 1 + 1$ means the account of the decay of the phonon from the second branch to two phonons from the acoustic branch and the inverse process of fusion. Actually only some parts of the corresponding branches can participate in these three-phonon interactions. Indeed, the processes with two phonons from the dispersionless optical modes and one phonon from the acoustic or from the first optical mode are allowed only for the small k of the latter mode. All other processes between such phonons are forbidden. Thus we conclude that phonons with small wavevectors do not contribute to these three-phonon processes and, therefore, such phonons have no broadening at all. This observation conforms with known results of inelastic neutron scattering measurements close to the strong Bragg peaks, which

show that there is characteristic wavevector q_{1c} of the order of $(0.3-0.5)$ Å^{-1}, such that only for $q > q_{1c}$ do the sound modes exhibit broadening [4–7].

4.1. Basic model

Just to illustrate our calculation scheme, let us first consider the elementary cell with two atoms, 1 and m. The allowed three-wave processes depend strongly on the value of m. For $m = 3$ the only possible anharmonic process is the decay of the optical phonon with $k = 0$ and $\omega = \omega_0$ into the two phonons with $\omega = \omega_0/2$. For smaller m there is a finite k region within the optical mode where the decay is allowed. To study the three-wave phenomena quantitatively one has to start with the vibrational Hamiltonian of the system including third-order anharmonic terms. The Hamiltonian can be written as

$$H = \sum_s \int \mathrm{d}k \left(a_s^*(k,t)\omega_s(k)a_s(k,t) + \sum_{s_1,s_2} \int \mathrm{d}k_1 V (a_s^*(k,t)a_{s_1}^*(k_1,t)a_{s_2}(k+k_1,t) + \text{c.c.}) \right). \tag{4.1}$$

Here a_s^*, a_s are creation or annihilation operators of the corresponding phonons (see, e.g., [24] for more details), V is the three-wave coupling potential, the integration is performed over the first Brillouin zone, c.c. means the complex conjugated contribution, and the summation is performed over all branches of the phonon spectrum. For the simplest model with two particles in the elementary cell, these are one acoustic and one optical branch.

We calculate the first anharmonic corrections to the phonon spectrum. Since the expansion in the Hamiltonian (4.1) is over the gradients of the atomic displacements, the triple phonon interaction vertex V can be presented as $V = \lambda\sqrt{\omega\omega_1\omega_2}$. Indeed the creation and annihilation operators a_s^*, a_s entering (4.1) expressed in terms of atomic displacements contain normalization coefficients $\propto\sqrt{\omega}$, where ω is the frequency of the corresponding mode. The interaction vertex λ has also some smooth dependence on the wavevectors [24] which, however, can be found only numerically. Therefore, to illustrate the essential physics by a simple picture, in the paper we neglect this dependence, and in what follows only the dimensionless anharmonic coupling constant $g = T\lambda^2$ will be used (T is temperature).

According to the general principles of quantum statistical physics [24], the probability of a phonon decay, i.e., the vibrational mode broadening, can be calculated self-consistently from the Hamiltonian (4.1). The mode widths $\gamma_{1,2}$ are determined by the following Born integral equations:

$$\begin{aligned}
\gamma_1(k,\omega_1) &= g\omega_1(k) \int \mathrm{d}k' \frac{(\omega_2(k+k') - \omega_1(k'))(\gamma_1(k') + \gamma_2(k+k'))}{(\omega_1(k) + \omega_1(k') - \omega_2(k+k'))^2 + (\gamma_1(k') + \gamma_2(k+k'))^2}, \\
\gamma_2(k,\omega_2) &= g\omega_2(k) \int \mathrm{d}k' \frac{(\omega_1(k') + \omega_1(k-k'))(\gamma_1(k') + \gamma_1(k-k'))/2}{(\omega_2(k) - \omega_1(k') - \omega_1(k-k'))^2 + (\gamma_1(k') + \gamma_1(k-k'))^2}.
\end{aligned} \tag{4.2}$$

Here subscripts 1 and 2 label acoustic and optic mode respectively, and the (4.2) are the integral equations to calculate self-consistently the mode broadening $\gamma_{1,2}$ provided the mode harmonic dispersion laws $\omega_{1,2}$ are known. Note also that the system of equations (4.2) is not symmetric with respect to $1 \leftrightarrow 2$ exchange, as it should be, since there is not any specific symmetry relation between acoustic and optic modes. Our main concern here is the case where the phonon broadening is rather large, therefore the thermal phonon excitations giving dominate contributions into the broadening should be thermally occupied, i.e., $T \geqslant T_D$ (T_D is Debye temperature), as is the case in the experimental inelastic neutron scattering investigations [5–7]. In the condition $T \geqslant T_D$ we replace the Bose energy level occupation factor $(\exp(\hbar\omega/T) - 1)^{-1}$ by the Boltzmann distribution function $T/\hbar\omega$ in the high-temperature limit. The solutions to

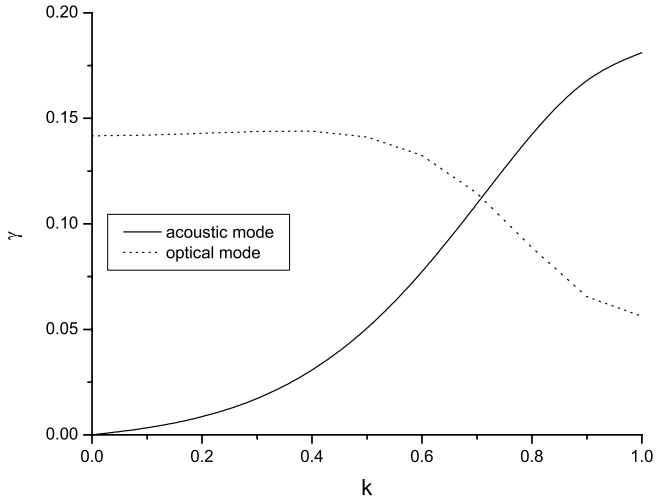

Figure 5. Phonon broadening calculated self-consistently from (4.2) (the mass ratio is 1:2.81 and the three-wave interaction vertex $g = 0.05$).

these equations can be easily found numerically, and we present the results in figure 5. One might think that equations (4.2) do not contain any QC-specific feature of the system, but this is only partially true. In fact the mode broadening (4.2) is determined by the key QC property, namely, a finite band of almost dispersionless optic modes interacting with the acoustic phonon. On the same footing the aforesaid statement is applied in our approach to any system with a non-simple unit cell. Indeed the low-lying optical modes from approximant crystals might be practically indistinguishable from quasi-local modes. At a given mass ratio m the broadening depends on the mode coupling parameter g, i.e., it is non-universal. It is also worth noting quite peculiar behaviour for the optical mode broadening decreasing for $k > 0.5$. The physics behind this can be rationalized as follows. For a given mass ratio about 2.8 the conservation laws prohibit three-wave interactions of the type $1 + 1 \leftrightarrow 2$ for optical phonons with wavevectors $k > 0.5$. This broadening reduction phenomenon is even more pronounced for the smaller coupling constant, as is demonstrated below in figure 7.

Figure 6 illustrates the three-wave broadening for a relatively large anharmonic coupling, $g = 0.05$. The results in this strong coupling case can be fitted by an ω^3 law. For a small coupling constant the broadening law is quite different, as we show in figure 7, where $g = 0.005$. In both cases the mass ratio is 1:2.81, which mimics the two kinds of i-QC we described above. Figures 6 and 7 manifest clearly that ω^3 dependence does not hold for small anharmonic coupling, and besides the figures show the difference between the regions of parameters corresponding to forbidden and allowed three-wave processes. Note also, that the three-wave anharmonic coupling at length scales relevant in (4.2) may be different from anharmonic contributions measured by macroscopic methods sensitive to anharmonic effects, for example, linear thermal expansivity, excess (in comparison to Debye law) specific heat, and various Grüneisen parameters [25, 26], or thermal conductivity [27, 28].

We have already shown in section 2 that the main structure of the vibration spectrum for quasi-periodic chains can be obtained in practice by considering very short approximants to infinite chains. For the Fibonacci chain, the reasonable size approximant contains five particles in the elementary cell, which is with our choice of masses $(m, 1, m, m, 1)$. Note that the same statement is true for electronic spectra [22, 23] as well. Although the generalization

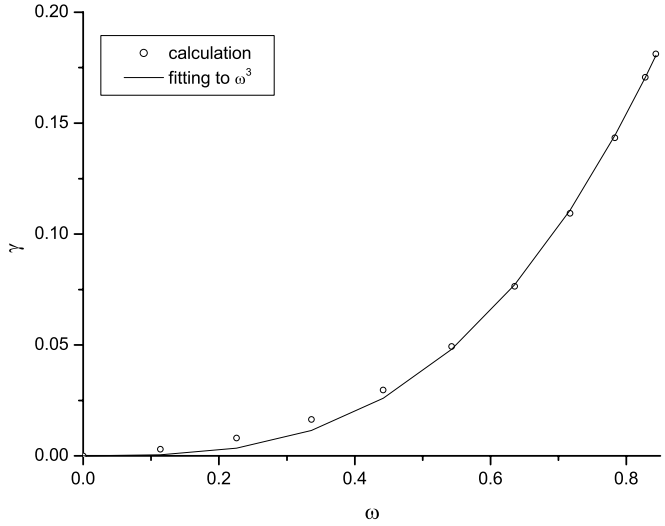

Figure 6. Acoustic phonon broadening as a function of ω (the solid line is the function $0.3\omega^3$; the parameters are the same as in figure 5).

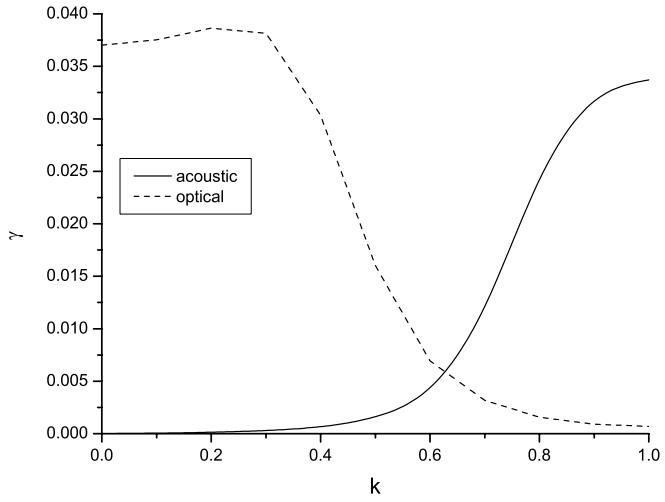

Figure 7. Phonon broadening calculated self-consistently from (4.2) (the mass ratio is 1:2.81 and the three-wave interaction vertex $g = 0.005$).

of the above analysis and results for two particles in the elementary cell to the unit cells with five atoms is conceptually straightforward, it deserves some precaution, as it implies tedious and bulky calculations, which could be done analytically only under certain rather restrictive approximations. Appendix A to the paper contains basic methodical details and equations necessary for these calculations, and besides it gives a way to construct a regular method for calculating higher-order perturbative corrections. In figure 8 we present the results of this analysis for the five-atom elementary cell. Only the main three-wave processes $1 + 1 \leftrightarrow 2$, $2 + 2 \leftrightarrow 3$, $1 + 3 \leftrightarrow 4$, $1 + 4 \leftrightarrow 5$, $2 + 3 \leftrightarrow 5$ are taken into account at the computation, and besides, for the sake of simplicity and having in mind published inelastic neutron scattering

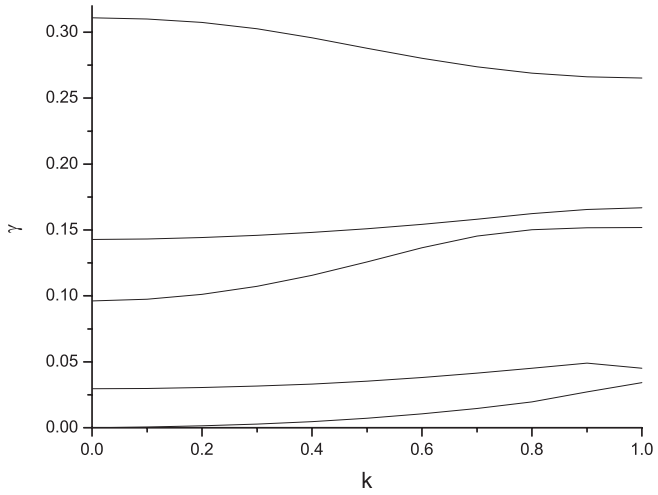

Figure 8. Self-consistent solution of equations (A.1) for the mass ratio 1:2.81 and parameter $g = 0.005$. Solid lines in this figure for $k = 0$ are branches with numbers 1, 2, 3, 4, 5. The width of the lowest acoustic mode tends to zero at $k \to 0$; the widths for the higher energy branches 3, 4, 5 are of the same order of magnitude.

experimental data [4, 5, 3, 6, 7], all in the range above the Debye temperature, we assume the Boltzmann statistics of the vibrational excitations.

Figure 8 shows that the width of the acoustic branch tends to zero for small wavevectors, and that the higher energy mode broadening (3, 4, 5) is in the same range of magnitude (of the order of 0.15 in our dimensionless units). Note that characteristic inter-mode spacing (i.e., eigenfrequency differences) is about 0.3 in the same units (see section 2). To summarize:

- Near the gaps due to resonances between acoustic and optic modes the sound mode can no longer be described as a single excitation.
- Large broadening of the acoustic phonon modes is related to the three-wave mechanism.
- There are at least two main reasons why three-phonon processes lead to much more noticeable contributions to sound absorption in QCs (more precisely in systems with non-simple unit cells) in comparison with conventional crystals. First for the QC there is a dense set of umklapp vectors, and second there are almost dispersionless optic modes possessing finite widths, and a large phase volume in reciprocal space is available for acoustic phonons interacting with the optical modes.
- The very existence of several quiet broad optical modes in QCs can be understood as an illustration that in QCs there are many ways in which the neighbouring configurations can be arranged; as a result a single mode, which initially was the same for all configurations, becomes a band of the modes.
- This noticeable broadening might be a reason why no forbidden gaps have been observed experimentally.

A few more words on umklapp processes seem appropriate here. The total momentum of any set of interacting particles in a periodic crystal needs only be conserved to within a wavevector from the reciprocal lattice, and these umklapp processes open further scattering channels where the momentum of the particles in the initial state is different from that of the final state. In a QC its reciprocal space contains all the necessary wavevectors to match any required frequency conversion processes. However, this striking fact is almost irrelevant for linear, i.e., one-mode,

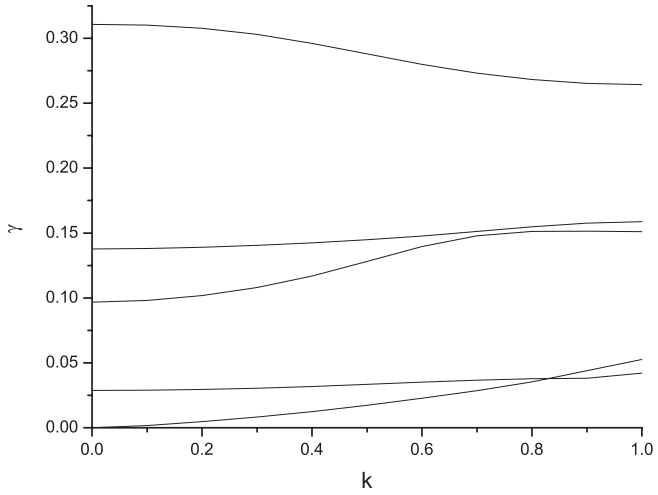

Figure 9. Vibrational mode broadenings for the $N = 5$ approximant. The mass ratio is 1:2.81 and the coupling parameter is $g = 0.005$.

phenomena. Evidently it is not the case for non-linear processes, like three-wave interaction, which can be enhanced noticeably in quasi-periodic systems.

4.2. Refinement of the basic model

The results presented in the previous subsection can be extended in many ways. First, for the sake of a sceptical reader we have to admit that strictly speaking our calculations are not self-consistent ones. Indeed in our approach (4.2) (see also (A.1) in appendix A) we have taken into account only three-wave processes which are not forbidden in the zero-temperature limit. In other words this means that there is no bare phonon mode broadening. For finite temperatures and non-zero bare phonon decay, the other processes could be also relevant, and the most important processes are $1 + 1 \leftrightarrow 1$, because the spectrum of acoustic phonons is approximately linear for small wavevectors, which always allows three-phonon interactions. Therefore in the case of finite temperatures, we have to add the contributions corresponding to these $1 + 1 \leftrightarrow 1$ processes into the right-hand side (rhs) of the first equation (4.2) or for the five-particle elementary cell into the rhs of (A.1). We present in figure 9 the phonon broadening with such a contribution taken into account for the coupling vertex $g = 0.005$. A nice feature of this contribution is that the shape of the acoustic branch width turns out to be almost independent of g for the interaction constant g larger than the threshold, which is about 0.005; see figure 10. One note of caution is in order here. In the previous subsection we replaced the Bose distribution function $(\exp(\hbar\omega/T) - 1)^{-1}$ by the classical occupation factor $T\hbar/\omega$. Luckily the acoustic branch broadening keeps its shape depicted in the figure 10 up to a temperature larger than the maximum phonon energy in the acoustic branch. Thus our approximation holds as well in a quite broad range of temperatures.

This universal contribution into the acoustic mode broadening can also be analysed analytically, and it illustrates several characteristic features of the phenomenon. We believe that the phonon width is significantly smaller than its frequency. To simplify this consideration we assume also that the widths of the optical modes do not depend on ω or k. Experimental data and our numerical investigations show that optical phonon widths indeed only very weakly depend on the wavevectors. Replacing in the first equation in (A.1) $\omega_1(k) \sim c|k|$, where c is

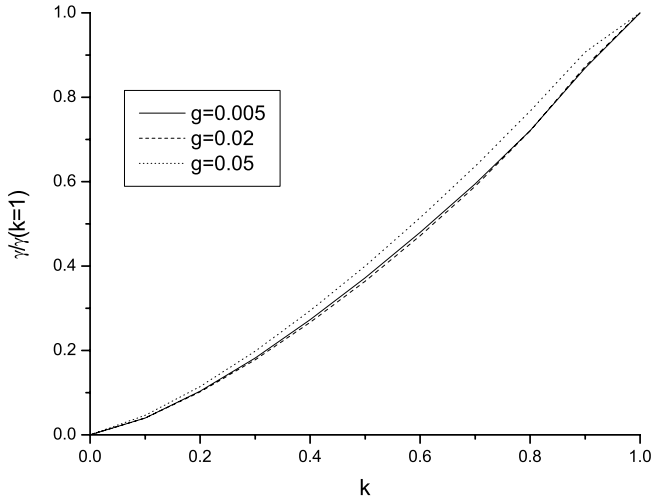

Figure 10. Acoustic mode broadening for the $N = 5$ approximant. The mass ratio is 1:2.81 and the coupling parameter values are indicated in the figure.

the speed of sound, and assuming that the width γ is small in comparison with the frequency ω, we face solving the integral equation

$$\gamma_1(k) = k^2\left(c_2 + c_1\int_0^1 \mathrm{d}q \frac{\gamma_1(q)+\gamma_1(q+k)}{c^2(|k|+|q|-|k+q|)^2+(\gamma_1(q)+\gamma_1(q+k))^2}\right)$$
$$= k^2\left(c_2 + c_1\int_0^1 \mathrm{d}q \frac{1}{\gamma_1(q)+\gamma_1(q+k)}\right), \tag{4.3}$$

where c_1 and c_2 are numerical coefficients. The form of the solution to equation (4.3) can be found straightforwardly and it reads

$$\gamma_1(k) \simeq c_1 k + c_2 k^2. \tag{4.4}$$

The approximate equality in (4.4) is obtained after the first iteration in (4.3). Thus we end up with the following universal analytical form for the acoustic mode width: $\gamma_1(k) = c_1 k + c_2 k^2$. This simple expression fits very well the function $\gamma_1(k)$ computed numerically (see figure 11). In order to provide a more complete account of the vibrational broadening phenomena, a similar analysis has been performed to include self-consistently the potentially relevant processes $n \leftrightarrow n+1$ (n is the vibrational branch number, and $n = 1$ corresponds to the acoustic mode). We closely follow the same procedure as above for the $1 \leftrightarrow 1+1$ broadening and thus skipping all details present only the results in figure 12. It turns out that these new processes have little effect on the acoustic branch width, and the broadenings of all other branches only weakly depend on the wavevector and increase monotonically with the branch number. The result justifies the assumptions made above, and proves that our model includes all ingredients necessary to capture the correct broadening effects in the Fibonacci chain for $T > T_\mathrm{D}$.

4.3. Self-consistent expansion over the parameter $\epsilon = 1 - 1/m$

We investigated the Fibonacci lattice based on the golden ratio as an example of the quasi-periodic 1D systems. To confront our results with experimental data for well-studied i-QCs we have taken the mass ratio to be $m = 3$. There are many other non-periodic structures which are nonetheless fully deterministic and in this sense highly ordered. Qualitatively one can

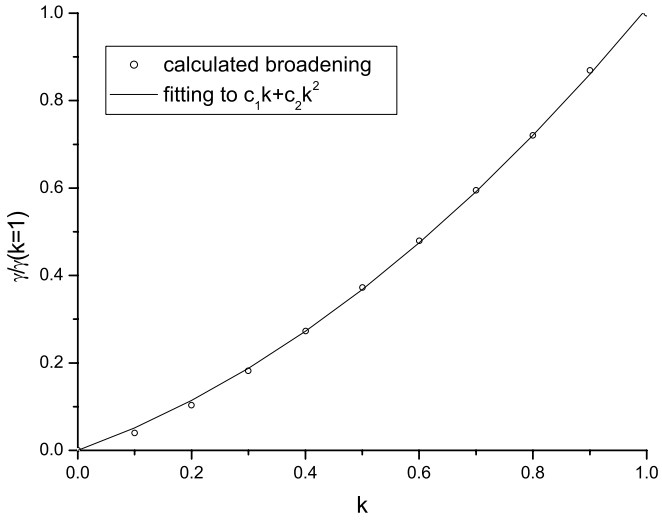

Figure 11. Numerically computed acoustic mode broadening for the $N = 5$ approximant and its theoretical fit by (4.3).

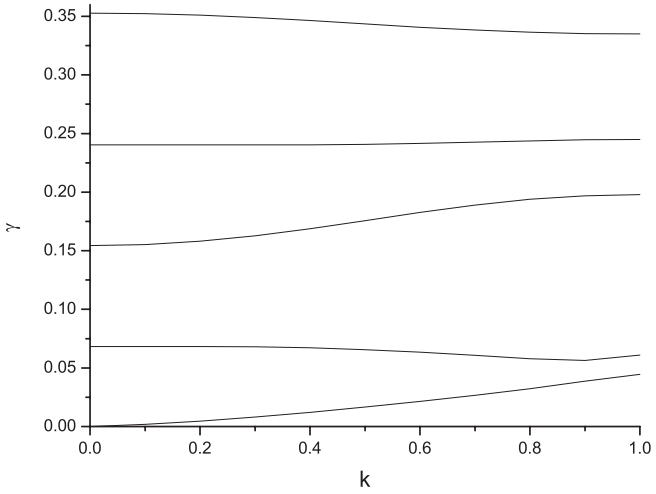

Figure 12. Vibrational mode broadenings with the processes $n \leftrightarrow n+1$ taken into account ($N = 5$ approximant and for the mass ratio 1:2.81).

also expect the same behaviour in 1D incommensurate systems. With this remark in mind it is interesting and instructive to extend the analysis of the previous section to a quasi-periodic system with the mass ratio m chosen to make use of the smallness of the parameter $\epsilon = 1-1/m$. If this assumption is granted we can apply a regular expansion over the small ϵ which allows us to study even the infinite chain.

To move further on smoothly let us recall the characteristic features of the Fourier spectrum for a periodically repeated finite Fibonacci block (remember that the length of the elementary cell is a Fibonacci number also). According to the Nyquist theorem (see, e.g., [29]) for N particles in the elementary cell one can determine only $N/2$ independent Fourier harmonics. The absolute value of each Fourier amplitude is an even function of its wavenumber. The zero

wavenumber harmonic has the largest amplitude. The next largest amplitude harmonics have numbers N_1 and $N - N_1$, with the ratio N_1/N close to the golden ratio $N_1/N \sim 0.62$. The next (by their amplitudes) harmonics have the wavenumbers $N_2 \sim 0.62N_1$ and so on. For example, for $N = 21$ the wavenumbers of the highest harmonics are $0, 8, 5, \ldots$. Evidently the amplitudes of all harmonics with non-zero wavenumbers are proportional to the small parameter ϵ; the corresponding proportionality coefficients are approximately constant and the constant is smaller than one. The amplitude ratio of the different harmonics is independent of the small parameter ϵ, and for the first two main harmonics (except the zero harmonic) this ratio is about 0.38.

Armed with this knowledge we can consider the phonon spectrum of such a system. For N particles in the elementary cell we get the spectrum with one acoustic and $N - 1$ optical branches. The gaps between the branches are determined by the amplitudes of corresponding Fourier harmonics. The amplitude of the harmonic, say, with the wavenumber K determines two spectral gaps with the numbers K and $N - K$ respectively. Noting that the sum of these two gaps is approximately equal to the amplitude of this harmonic, we arrive at the conclusion that the vibrational spectrum of the Fibonacci chain possesses the sequence of the gaps, and the value of the gap depends on its wavenumber and on the parameter ϵ. In the limit $\epsilon \to 0$ all gaps also tend to zero. The chain turns into the crystalline Bravais lattice with only one particle in its elementary cell and only one acoustic phonon branch. For finite but small values of the parameter ϵ the difference between the phonon spectra of the quasi-periodic system under consideration and the corresponding Bravais lattice should be also small. To be more specific let us focus on the simplest non-Bravais system with three particles in the elementary cell. The main feature of this non-Bravais lattice is that the length of the Brillouin zone is three times smaller than for its Bravais counterpart, and besides there are two additional non-zero Fourier harmonics. The acoustic branch of the non-Bravais lattice practically coincides with the corresponding part (one third) of the acoustic branch of the Bravais lattice. However, the optical branches in the non-Bravais lattice spectrum are significantly different. Let us denote by q_0 the size of the Brillouin zone for the Bravais lattice. For the optical modes we easily get that $\omega_2(k) \sim \omega_B(2q_0/3 - k)$ and $\omega_3(k) \sim \omega_B(k - 2q_0/3)$, where ω_B is the only phonon frequency in the Bravais lattice. Three-wave interaction in the Bravais lattice is determined by a certain vertex λ_3, which is supposed to be not very different from the similar triple interaction vertex between the acoustic phonons for the non-Bravais lattice. However, in the non-Bravais case we have to consider also all other interactions which include the optical phonons. We denote the corresponding vertex $\lambda_4 a(q_i)$, because it describes in fact the four-wave coupling, and $a(q_i)$ is the Fourier amplitude of the density modulation at the wavevector q_i. Actually the vertex λ_3 can also be reduced to $\lambda_4 a(q_0)$, and therefore the natural estimate for the vertices is $\lambda_4 a(q_i)/\lambda_3 \sim a(q)/a(0) \sim \epsilon$.

The number of wavevectors q entering the vibrational thermal broadening is equal to the number of optical modes. Thus for our simple case with three particles in the elementary cell we have to deal with two vectors, and their Fourier amplitudes are equal and proportional to ϵ. Furthermore the effective triple vertex in the main over ϵ approximation including all not forbidden processes can be written as

$$\lambda_{\text{eff}} = \lambda_3 \delta(k_1 + k_2 + k_3) + \sum_i \lambda_4 a(q_i) \delta(k_1 + k_2 + k_3 + q_i).$$

Finally the thermal vibrational mode broadening is determined by the square of this vertex. In a generic situation the different contributions into λ_{eff} do not interfere. Let us recall again that this conclusion is based on our assumption of $\epsilon \ll 1$, which is equivalent to saying that the amplitudes $a(q_i)$, are small, and non-small Fourier harmonics are included in the basic structure as we did above for the harmonic with the wavevector q_0.

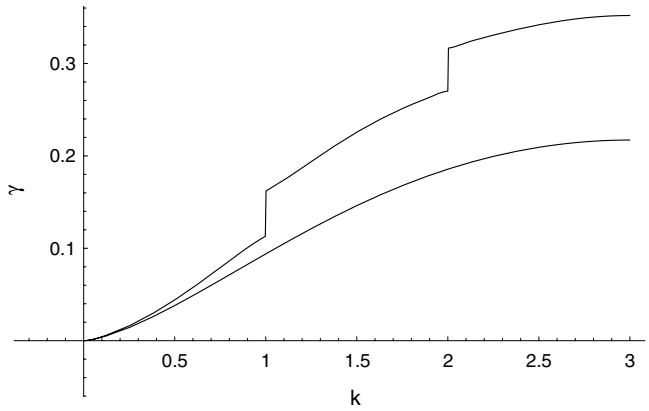

Figure 13. Comparison of the spectra for the Bravais system and its non-Bravais counterpart (the mass ratio is about 1:3): smooth line—the broadening in the 1D Bravais crystal; curve with the jumps—the broadening in the system with three particles in the elementary cell with the same interaction constant g as for the smooth line.

Now we can compare the thermal broadening for the Bravais and non-Bravais cases. The only three-wave process allowed in the Bravais lattice is evidently $1 \leftrightarrow 1 + 1$. For the non-Bravais case we have besides it also the three-wave processes related to the interaction vertex $\lambda_4 a(q_i)$. For our simplest case with three particles in the elementary cell $a(q_0/3) = a(2q_0/3)$ and both additional vertices coincide and are proportional to ϵ. One can see that the vibrational broadening for the non-Bravais case always exceeds the broadening in its Bravais counterpart. The corresponding difference of both widths $\gamma_3 - \gamma_B$ is proportional to the value $\sum_i a(q_i)^2$ (for the sake of simplicity we consider λ_4 to be a constant). We present the results in figure 13 for $\lambda_3 = 0.05$ and $\lambda_4 = 0.66\lambda_3$ ($\epsilon \sim 2/3$). The qualitative inescapable message of this is that the phonon broadening is always larger for a non-simple elementary cell in comparison to the corresponding simple Bravais elementary cell.

5. Conclusion

We have examined one important (and overlooked in previous investigations) aspect of QC vibration spectra, namely, three-wave anharmonic line broadening. Our model chain is constructed from particles with masses 1 and m following the Fibonacci inflation rule. As the length of the pattern goes to infinity, the ratio between the total number of elements of different components approaches a constant value. The eigenmode spectrum depends crucially on the mass ratio m. For $m = 3$, which roughly mimics i-QC AlPdMn, there are three almost dispersionless optic modes separated from the acoustic mode by three large gaps. For $m = 1/3$, which mimics ZnMgY i-QCs, there is one dispersionless optic mode and one acoustic mode. All calculations are performed self-consistently at finite temperatures $T > T_D$ within the regular expansion over the three-wave coupling constant. We have demonstrated that this problem can be treated as well in the framework of the perturbation theory over the parameter $1 - 1/m$, which may be formally considered as a small parameter. We have found noticeable three-wave anharmonic contributions into the mode broadening. At a given mass ratio m the broadening depends on the mode coupling constant, and for relatively strong coupling, is proportional to k^3, where k is the mode wavevector. The need of an exponent smaller than 4 (which is often attributed to Rayleigh scattering in disordered materials [8, 9]) of the power law

k-dependent broadening was indicated also in [20] in order to fit the thermoconductivity data in AlMnPd i-QC. We have shown that the line broadening dependence on mode wavevector is not a universal one. For a coupling parameter higher than $g = 0.005$ the exponent of the power law of the acoustic mode width becomes smaller than 3, and for very small coupling this kind of power-law fitting becomes inadequate. We have demonstrated that robust features of the vibrational spectra of 1D Fibonacci chain will carry over to 2D and 3D cases by extending our approach into 3D systems. We have shown that in the intermediate range of mode coupling constants, three-wave broadening depends universally on frequency ω and scales as $c_1\omega+c_2\omega^2$, where c_1 and c_2 are constants.

It is instructive to compare these predictions with the results known for standard (i.e., possessing simple Bravais unit cells) crystalline materials, where the inelastic anharmonic processes lead to a temperature-dependent linewidth which scales as k^2, whereas elastic scattering of the Bloch-like waves by the static inhomogeneities leads to a temperature-independent linewidth proportional to k^4 in 3D systems. Our important qualitative conclusion is that for a system with a non-simple elementary cell phonon spectrum broadening is always larger than that for a system with a primitive cell, provided all other characteristics are the same.

Although our model is a toy model in the sense of caricaturing some of the physical features of quasicrystals, it is capable of providing both qualitative and quantitative predictions for a variety of measured quantities, and establishes the properties of the vibrational spectra associated with generic features of any system with a non-simple unit cell.

Acknowledgments

We thank M de Boissieu and R Currat for the numerous discussions inspired this work. It is our pleasure also to acknowledge helpful discussion with Dr A Kozhekin. One of us (EIK) acknowledges support from INTAS (under No. 01-0105) Grants.

Appendix A

The system of equations for phonon line broadening in the five-particle approximant to the infinite Fibonacci chain reads

$$\gamma_1(k,\omega_1) = g\omega_1(k)\int \mathrm{d}k'\left(\frac{(\omega_2(k+k')-\omega_1(k'))(\gamma_1(k')+\gamma_2(k+k'))}{(\omega_1(k)+\omega_1(k')-\omega_2(k+k'))^2+(\gamma_1(k')+\gamma_2(k+k'))^2}\right.$$
$$+\frac{(\omega_4(k+k')-\omega_3(k'))(\gamma_3(k')+\gamma_4(k+k'))}{(\omega_1(k)+\omega_3(k')-\omega_4(k+k'))^2+(\gamma_3(k')+\gamma_4(k+k'))^2}$$
$$\left.+\frac{(\omega_5(k+k')-\omega_4(k'))(\gamma_4(k')+\gamma_5(k+k'))}{(\omega_1(k)+\omega_4(k')-\omega_5(k+k'))^2+(\gamma_4(k')+\gamma_5(k+k'))^2}\right)$$

$$\gamma_2(k,\omega_2) = g\omega_2(k)\int \mathrm{d}k'\left(\frac{\omega_1(k')(\gamma_1(k')+\gamma_1(k-k'))}{(\omega_2(k)-\omega_1(k')-\omega_1(k-k'))^2+(\gamma_1(k')+\gamma_1(k-k'))^2}\right.$$
$$+\frac{(\omega_3(k+k')-\omega_2(k'))(\gamma_2(k')+\gamma_3(k+k'))}{(\omega_2(k)+\omega_2(k')-\omega_3(k+k'))^2+(\gamma_2(k')+\gamma_3(k+k'))^2}$$
$$\left.+\frac{(\omega_5(k+k')-\omega_3(k'))(\gamma_3(k')+\gamma_5(k+k'))}{(\omega_2(k)+\omega_3(k')-\omega_5(k+k'))^2+(\gamma_3(k')+\gamma_5(k+k'))^2}\right)$$

$$\gamma_3(k,\omega_3) = g\omega_3(k)\int \mathrm{d}k'\left(\frac{\omega_2(k')(\gamma_2(k')+\gamma_2(k-k'))}{(\omega_3(k)-\omega_2(k')-\omega_2(k-k'))^2+(\gamma_2(k')+\gamma_2(k-k'))^2}\right. \tag{A.1}$$
$$+\frac{(\omega_4(k+k')-\omega_1(k'))(\gamma_1(k')+\gamma_4(k+k'))}{(\omega_3(k)+\omega_1(k')-\omega_4(k+k'))^2+(\gamma_1(k')+\gamma_4(k+k'))^2}$$
$$\left.+\frac{(\omega_5(k+k')-\omega_2(k'))(\gamma_2(k')+\gamma_5(k+k'))}{(\omega_3(k)+\omega_2(k')-\omega_5(k+k'))^2+(\gamma_2(k')+\gamma_5(k+k'))^2}\right)$$
$$\gamma_4(k,\omega_4) = g\omega_4(k)\int \mathrm{d}k'\left(\frac{(\omega_1(k')+\omega_3(k-k'))(\gamma_1(k')+\gamma_3(k-k'))}{(\omega_4(k)-\omega_1(k')-\omega_3(k-k'))^2+(\gamma_1(k')+\gamma_3(k-k'))^2}\right.$$
$$\left.+\frac{(\omega_5(k+k')-\omega_1(k'))(\gamma_1(k')+\gamma_5(k+k'))}{(\omega_4(k)+\omega_1(k')-\omega_5(k+k'))^2+(\gamma_1(k')+\gamma_5(k+k'))^2}\right)$$
$$\gamma_5(k,\omega_5) = g\omega_5(k)\int \mathrm{d}k'\left(\frac{(\omega_1(k')+\omega_4(k-k'))(\gamma_1(k')+\gamma_4(k-k'))}{(\omega_5(k)-\omega_1(k')-\omega_4(k-k'))^2+(\gamma_1(k')+\gamma_4(k-k'))^2}\right.$$
$$\left.+\frac{(\omega_2(k')+\omega_3(k-k'))(\gamma_2(k')+\gamma_3(k-k'))}{(\omega_5(k)-\omega_2(k')-\omega_3(k-k'))^2+(\gamma_2(k')+\gamma_3(k-k'))^2}\right).$$

Here only the main three-wave processes $1+1 \leftrightarrow 2$, $2+2 \leftrightarrow 3$, $1+3 \leftrightarrow 4$, $1+4 \leftrightarrow 5$, $2+3 \leftrightarrow 5$ are taken into account and, besides, we assume classical statistics for the vibrational excitations. The self-consistent solution to these equations, shown in figure 8 for the mass ratio 1:2.81 and parameter $g = 0.005$, qualitatively resembles experimentally observed spectra. Note, however, that the line broadening dependence on wavevectors turns out to be not a universal one. The acoustic mode width for the non-linear coupling parameter $g = 0.005$ can be fitted by the power law $\omega \propto k^3$, but for higher values of g the exponent in this power law decreases, and for very small coupling power-law fitting is not possible anymore.

Appendix B

The main problem to treat theoretically mode broadening in 3D quasicrystals is related to the fact that there is no well-defined Brillouin zone. Luckily, for finite temperature three-wave line broadening, the integrals entering the expression for the broadening only weakly depend on the region in the vicinity of the boundary of the pseudo-Brillouin zone. Having in mind highly symmetric elastic properties of the i-QCs, one can perform this integration over an appropriate chosen spherical volume. Indeed, despite (at least partially) contradictory results of experimental investigations [3, 7], and [25] a few conclusions about the following qualitative features of the phonon broadening in 3D systems seem inescapable:

- sound velocity is approximately isotropic;
- the broadening for wavevectors 0.3–0.5 A^{-1} is also isotropic;
- phonon lines have almost Lorentzian shapes.

Note also that the icosahedron and inverse dodecahedron (the main building blocks for any i-QCs) are the most isotropic perfect polyhedra. The broadening due to the three-phonon interactions is determined by the integral which has singularity along the line corresponding to the zero angle between the wavevectors. All these features mean that the approximation which replaces the first Brillouin zone by a sphere is a quite reasonable one. Having this in mind,

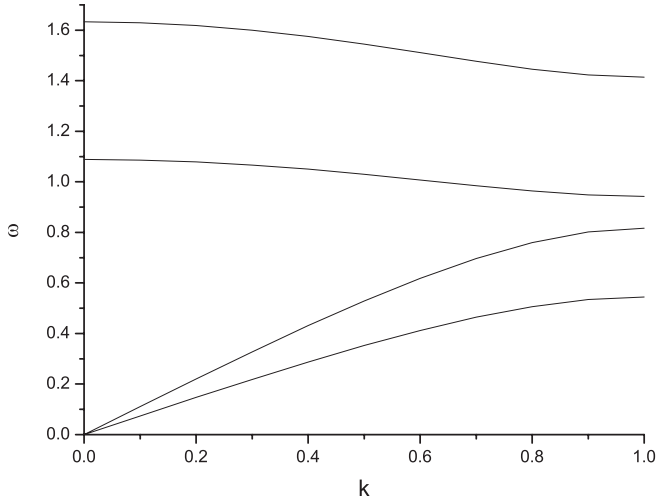

Figure B.1. Phonon spectrum for the 3D isotropic model of i-QCs with three acoustic branches and three optical branches (transverse modes are degenerate).

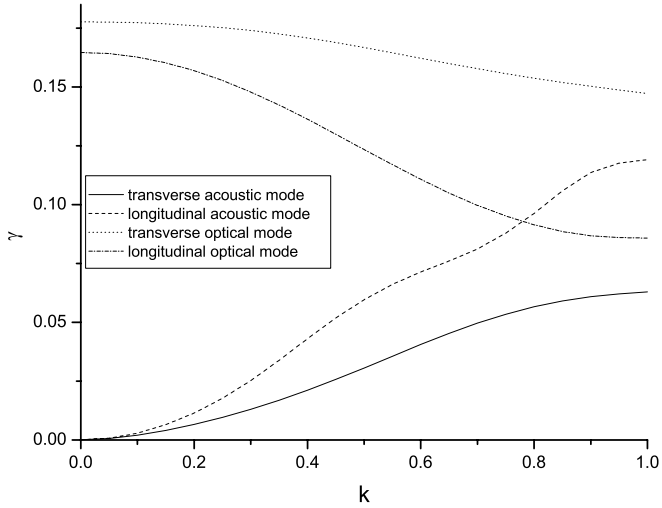

Figure B.2. The broadening of the phonons for the same model as in figure B.1, and for $\gamma/\omega \sim 0.16$.

we calculate the broadening for the simplest case of an isotropic system with the reciprocal q-space limited by the sphere $|\mathbf{q}| = q_0$ and with only a one-phonon branch

$$\gamma(q) = g\omega(q)^2 \int_0^{q_0} \mathrm{d}k\, k^2 \int_{-1}^{1} \mathrm{d}t \left(\frac{(\gamma(\mathbf{k}) + \gamma(\mathbf{q}-\mathbf{k}))/2}{(\omega(\mathbf{q}) - \omega(\mathbf{k}) - \omega(\mathbf{q}-\mathbf{k}))^2 + (\gamma(\mathbf{k}) + \gamma(\mathbf{q}-\mathbf{k}))^2} + \frac{\gamma(\mathbf{k}) + \gamma(\mathbf{q}+\mathbf{k})}{(\omega(\mathbf{q}) + \omega(\mathbf{k}) - \omega(\mathbf{q}+\mathbf{k}))^2 + (\gamma(\mathbf{k}) + \gamma(\mathbf{q}+\mathbf{k}))^2} \right). \tag{B.1}$$

Because everything is isotropic for this case, one has $\gamma(\mathbf{k}) = \gamma(k)$ and $\gamma(\mathbf{q} \pm \mathbf{k}) = \gamma(\sqrt{q^2 + k^2 \mp 2qk\cos\hat{kq}})$. The integration above is performed over the region $|\mathbf{k}| < q_0$. Thus we choose $q < q_0$, and if $|\mathbf{q} \pm \mathbf{k}|$ occurs to be larger than q_0, it must be replaced with

$2q_0 - |\mathbf{q} \pm \mathbf{k}|$. The first term in the rhs corresponds to the decay of a phonon with the wavevector $\mathbf{q}$, the second term describes the fusion of this phonon with the phonon with the wavevector $\mathbf{k}$, and to be specific the phonon spectrum is taken as $\omega(q) = \omega_0 \sin(\frac{\pi q}{2q_0})$. The generalization for a larger number of particles in the elementary cell is straightforward. In the case of two particles, the phonon spectrum consists of three acoustic and three optic branches, and due to the isotropy of the system the transverse branches should be degenerate. The solution to the corresponding equations can be found as above. The results for the eigenfrequencies are presented in figure B.1 and for the vibrational mode broadenings in figure B.2. Maximal frequencies for longitudinal acoustic and optic modes are 0.81 and 1.4 correspondingly, i.e., the ratio $\gamma/\omega(k = 1) \sim 1/7$, i.e., quite close to the neutron scattering experimental data [5–7]. The robust qualitative features of the broadening for both the longitudinal and transverse acoustic branches are very similar ones, and can be fitted as $c_1 k + c_2 k^2$. This answer is universal for the model, when the broadening is determined by only one three-wave interaction constant g.

References

[1] Cahn J W, Shechtman D and Gratias D 1986 *J. Mater. Res.* **1** 13
[2] Janot C 1992 *Quasicrystals: A Primer* (Oxford: Oxford Science)
[3] Bellissent R, de Boissieu M and Coddens G 1999 *Physical Properties of Quasicrystals* ed Z M Stadnik (Berlin: Springer)
[4] de Boissieu M, Boudard M, Bellissent R, Quilichini M, Hennion B, Currat R, Goldman A I and Janot C 1993 *J. Phys.: Condens. Matter* **5** 4945
[5] Boudard M, de Boissieu M, Kycia S, Goldman A I, Hennion B, Bellissent R, Quilichini M, Currat R and Janot C 1995 *J. Phys.: Condens. Matter* **7** 7299
[6] Dugain F, de Boissieu M, Shibata K, Currat R, Sato T J, Kortan A R, Suck J B, Hradil K, Frey F and Tsai A P 1999 *Eur. Phys. J.* B **7** 513
[7] Shibata K, Currat R, de Boissieu M, Sato T J, Takakura H and Tsai A P 2002 *J. Phys.: Condens. Matter* **14** 1847
[8] Courtens E, Foret M, Hehlen B, Rufflé B and Vacher R 2003 *J. Phys.: Condens. Matter* **15** 1281
[9] Rufflé B, Foret M, Courtens E, Vacher R and Monaco G 2003 *Phys. Rev. Lett.* **90** 095502
[10] Hafner J and Krajci M 1993 *J. Phys.: Condens. Matter* **5** 2489
[11] Hafner J, Krajci M and Michalkovic M 1996 *Phys. Rev. Lett.* **76** 2738
[12] Niizeki K 1989 *J. Phys. A: Math. Gen.* **22** 4295
[13] Niizeki K and Akamatsu T 1990 *J. Phys.: Condens. Matter* **2** 2759
[14] Janot C 1996 *Phys. Rev.* B **53** 181
[15] Quilichini M and Janssen T 1997 *Rev. Mod. Phys.* **69** 277
[16] Janssen T 2000 *Ferroelectrics* **236** 157
[17] Levine D, Lubensky T C, Ostlund S, Ramaswamy S and Steinhard P J 1985 *Phys. Rev. Lett.* **54** 1520
[18] Lubensky T C, Ramaswamy S and Toner J 1985 *Phys. Rev.* B **32** 7444
[19] Lu J P, Odugaki T and Birman J L 1986 *Phys. Rev.* B **33** 4809
[20] Kalugin P A, Chernikov M A, Bianchi A and Ott H R 1996 *Phys. Rev.* B. **53** 1445
[21] Kramer P and Neri R 1984 *Acta Crystallogr.* A **40** 580
[22] Roche S and Mayou D 1997 *Phys. Rev. Lett.* **79** 2518
[23] Roche S, Bicout D, Macia E and Kats E 2003 *Phys. Rev. Lett.* **91** 228101
[24] Landau L D and Lifshits E M 1981 *Physical Kinetics, Course of Theoretical Physics* vol 10 (New York: Pergamon)
[25] Swenson C A, Fisher I R, Anderson N E Jr, Canfield P C and Migliori A 2002 *Phys. Rev.* B **65** 184206
[26] Swenson C A, Lograsso T A, Ross A R and Anderson N E Jr 2002 *Phys. Rev.* B **66** 184206
[27] Chernikov M A, Ott H R, Bianchi A, Migliori A and Darling T W 1998 *Phys. Rev. Lett.* **80** 321
[28] Gianno K, Sologubenko A V, Chernikov M A and Ott H R 2000 *Phys. Rev.* B **62** 292
[29] Weaver H J 1983 *Applications of Discrete and Continuous Fourier Analysis* (New York: Wiley)